# Diffusion-weighted and diffusion-tensor imaging of normal and diseased uterus

Duygu Kara Bozkurt, Murat Bozkurt, Mehmet Ali Nazli, Ilhan Nahit Mutlu, Ozgur Kilickesmez

Duygu Kara Bozkurt, Depatment of Radiology, School of Medicine, Kafkas University, 36000 Kars,Turkey

Murat Bozkurt, Depatment of Obstetrics and Gynecology, School of Medicine, Kafkas University, 36000 Kars, Turkey

Mehmet Ali Nazli, Ilhan Nahit Mutlu, Ozgur Kilickesmez, Department of Diagnostic and Interventional Radiology, Istanbul Training and Research Hospital, 34098 Samatya, Istanbul, Turkey

Author contributions: Kara Bozkurt D and Kilickesmez O had equally contributed to this paper; Kara Bozkurt D and Bozkurt M wrote the paper; Nazli MA and Mutlu IN collected the figures and the literatures; Kilickesmez O approved the final version.

Conflict-of-interest statement: There's no conflict of interest.

Correspondence to: Ozgur Kilickesmez, MD, Associate Professor of Radiology, Department of Diagnostic and Interventional Radiology, Istanbul Training and Research Hospital, Org. Nafiz Gurman St, 34098 Samatya, Istanbul,
Turkey. okilickesmez@yahoo.com
Telephone: +90-532-7346196
Fax: +90-216-4693796

## Abstract

Owing to technical advances and improvement of the software, diffusion weighted imaging and diffusion tensor imaging (DWI and DTI) greatly improved the diagnostic value of magnetic resonance imaging (MRI) of the pelvic region. These imaging sequences can exhibit important tissue contrast on the basis of random diffusion (Brownian motion) of water molecules in tissues. Quantitative measurements can be done with DWI and DTI by apparent diffusion coefficient (ADC) and fractional anisotropy (FA) values respectively. ADC and FA values may be changed by various physiological and pathological conditions providing additional information to conventional MRI. The quantitative DWI assists significantly in the differentiation of benign and malignant lesions. It can demonstrate the microstructural architecture and celluler density of the normal and diseased uterine zones. On the other hand, DWI and DTI are useful for monitoring the treatment outcome of the uterine lesions. In this review, we discussed advantages of DWI and DTI of the normal and diseased uterus.

Key words: Magnetic resonance imaging; Diffusion weighted imaging; Diffusion tensor imaging; Uterus

Core tip: Diffusion weighted imaging (DWI) and diffusion tensor imaging (DTI) sequences greatly improved the diagnostic value of magnetic resonance imaging of the uterus with the additional benefits of functional information. They reflect the microstructural architecture and cellular density of the uterine zones and enable quantitative evaluation. Depending on this review, DWI and DTI appear to be applicable and reliable methods for demonstrating physiological changes of the uterus, benign and malignant characteristics of uterine zones

and monitoring the treatment outcome of the uterine diseases.

## INTRODUCTION

Diffusion weighted imaging (DWI) is a magnetic resonance imaging (MRI) sequence structured on the basis of diffusion (Brownian motion) of water molecules in the extracellular space and is being increasingly used to evaluate the female pelvis. The quantitative parameter acquired from DWI sequenceis the apparent diffusion coefficient (ADC) value. The basic factors affecting the ADC values are tissue structures, interactions between the molecules and cellular density. Thus, ADC is altered by many physiological and pathological conditions of the body[1].

Uterus is a fibromuscular solid organ under the effect of the hormones and is composed of three layers: the endometrial, the junctional and the myometrial zones. Physiological (menstrual cycle, menopausal period) fluctuations of these zones change the ADC values used in the evaluation of uterine abnormalities[1].

Diffusion is a multi-dimensional process, which occures in different values in different directions depending on the microstructure of the tissues. Since uterine myometrium is composed of smooth muscle bundles and connective tissue diffusion reflects aniso-tropic features. Though DWI gives information about the direction of diffusion and cellularity of the tissue, anisotropic characteristics of tissues can be assessed appropriately by diffusion tensor imaging (DTI). It can be used to detect water diffusion directionality which in turn shows the microstructural architecture of normal and diseased tissue. Fractional anisotropy (FA) is the main quantitative parameter obtained from DTI data. Initially DTI has been used to show and evaluate the integrity of white matter tracts in neuroradiology. With the improvement of the MRI hardware and softwares, fast imaging techniques, after the use of DWI also DTI was implemented to abdominal imaging for some of the abdominal organs like uterus. The initial researches have been published regarding DTI of the uterus specimens of the patients to whom hysterectomy was performed for medical reasons[2-4] and then *in vivo* on the uterus of the patients'[5].

Non-functional (conventional) MRI provides excellent anatomical information of the uterus, however, the morphological appearance still may not differentiate some of the benign and malignant uterine lesions[6]. DWI and DTI which provide functional information and when combined with conventional MRI become a complementary diagnostic tool for the uterus and giving more information for the differentiation and extension of benign and malignant lesions, and for the follow up of treatment outcome after uterine arterial embolization (UAE), oncological therapies[7].

In this paper, we aimed to focus on and review their diagnostic importance of the DWI and DTI techniques of the normal and diseased uterus.

## DWI AND DTI TECHNIQUE

Optimal MRI of the female pelvis should be performed on a high field strength MRI system (1.5 or 3 T) using local phased-array coils. High field strenght MRI and phased-array coils increase the signal-to-noise ratio, provide high resolution images for the DWI and DTI sequences. Besides development of ultra-fast pulse sequences such as echo-planar imaging and parallel imaging technique, enabled to prevent motion artefacts and consequently functional MRI of the female pelvis[8].

For conventional MRI T1, T2 and fat saturated T2-weighted fast spin echo sequences followed with pre and post contrast three dimensional gradient-recalled echo volumetric interpolated breath-hold sequences and three plane imaging is necessary which give morphological information about the uterine zones. The addition of DWI and DTI sequences to the conventional MRI gives functional data about the uterus.

DWI is acquired by the measurement of signal loss after a series of two motion-providing gradient (MPG) pulses with the addition of a 180° refocusing radio frequency pulse to both sides for enhancing the variations of molecular diffusion between tissues. The density of MPG pulses is shown by the *b*-value, an paramount criterion affecting the signal intensity of the DWI[7]. An appropriate *b* value is necessary for the female pelvic MRI.

In several studies, DTI has been used to demonstrate fiber structures of the *ex vivo* uterus, because of problematic conditions leading to artefacts such as body motions, heartbeat, intestinal and respiratory movements, and uterine peristalses[2-4]. Fiocchi *et al*[5], examined the DTI of *in vivo* uterus with a 3 T MRI using a 3D tractography algorithm and revealed that DTI is useful for imaging fibre architecture of *in vivo* human uterus.

## DWI AND DTI OF NORMAL UTERUS

In reproductive age groups, T1 and T2 signal inten-sity characteristics of the uterine zones (endometrial, junctional and myometrial) demonstrate variations during ongoing phases of the menstrual cycle and with menauposal status. Physiological fluctuations affect the normal ADC values used in the evaluation of uterine pathologies[6].

On conventional MRI, the endometrial zone reflects high signal on T2-weighted sequences, however not so high like urinary bladder and low signal intensity on

T1-weighted sequences[9]. The junctional zone is the inner band of the myometrium and shows a low signal intensity in comparison to myometrial zone on T2-weighted sequences, probably because of multifactorial reasons[10]. Existence of compact smooth muscles, low water content of the cells, and increased large nuclei are the contributing factors[10,11]. The outer band of myometrial zone shows high signal intensity on T2-weighted sequences than the junctional zone, with high cellular water content and low cell density[9].

The cervix is composed of three different cervical zones that may be identified on high-resolution T2-weighted sequences There is a hyperintense central layer, named endocervical canal including mucosa, secretions, and plica. Outside of this, there is a middle zone, that's characterized by hypointense signal on T2-weighted sequences because of fibrous stroma and smooth muscle. The peripheral exterior zone includes fibromuscular stroma reflecting low-intermediate signal on T2-weighted sequences[12].

The menstrual cycle includes of three different phases. The initial four days of the menstrual phase is nemed as menstruation. On the fifth day the proliferative (follicular) phase begins and continues until the ovulation which is estimated to occure on the 14th day of the menstrual cycle. The secretory (luteal) phase begins with ovulation and lasts on the first day of the next menstrual period[13].

Tsili *et al*[13], reported that the ADC values of the endometrial and myometrial zones were different in the three phases of the cycle (menstrual phase: 1.25 ± 0.27, 1.91 ± 0.35; proliferative phase: 1.39 ± 0.20, 1.72 ± 0.27; secretory phase: 1.50 ± 0.18, 1.87± 0.28, respectively). A wide variation of ADC values of normal endometrial and myometrial zones is detected during different periods of the menstrual cycle. These variations probably depends on the physiologic-histologic fluctuations[14]. In the menstrual period, periodic contractions of the spiral artery walls in the normal endometrial zone, cause interruption of the epithelium and rupture of the vessels. Endometrial discharge caused by the torn ends of venous structures, arteries and glands result in restricted diffusion in the endometrial zone during the menstrual phase. In the secretory phase, expanded uterine glands, prominent arteries in the normal endometrial zone, accompanied by less amount of cells in stratum basalis and higher interstitial fluid can be among the probable explanations for the higher ADC values[13].

Kido *et al*[1], examined both intraindividual and interindividual differences of the ADC values of the normal uterine zones during the phases of the menstrual cycle in young age group. In this report, the ADC values for myometrial and endometrial zones were lower in the menstrual phase in comparison to the periovulatory and the secretoryl phase, although significant variability among individuals was reported. These preliminary results must be kept in mind, that the menstrual cycle and individual differences in reproductive women should be taken into account during the interpretation of the ADC values of uterine zones[1].

Kuang *et al*[6], studied the ADCs of the normal uterine zones during different periods of the menstrual cycle between reproductive women with different ages. The ADC values of the uterine zones were statistically different from each other. Endometrial ADC values of the females in their 30 s were higher than the ones in their 20 s and in their 30 s in the midproliferative and midsecretory periods. Also the ADC values of endometrial zone for all age groups were lower in the midproliferative phase in comparison to midsecretory phase, however the ADC values of the myometrial and junctional zones were not statistically different between the phases and age groups. According to this study patient age, menstrual period and the zone evaluated should be taken into consideration during quantitative evaluation[6].

The relationship of the uterine zonal ADC values were investigated by Fornasa *et al*[15], between the different periods of the cycle. The ADC values of the endometrium calculated on the fifth day of the cycle were lower when compared with periovulatory ADC values at the fundus (mean 0.923 mm$^2$/s *vs* 1.256 × 10$^{-3}$ mm$^2$/s) and at the isthmus (mean 1.297 mm$^2$/s *vs* 1.529 × 10$^{-3}$ mm$^2$/s). Isthmic endometrial ADC values were higher than the fundal ADC values (mean 1.420 × 10$^{-3}$ mm$^2$/s *vs* 1.132 mm$^2$/s). These findings were statistically significant. Physiological fluctuations occurring in the ADC values of the endometrium of normal females should be kept in mind during the interpretation of the DW images of the patients[15].

DTI revealed two basic systems of fibers: circular and longitudinally oriented fibers as shown *ex-vivo*. Examination of the non cesarean scarred uteri showed anisotropy and fiber directions could be depicted[5]. Knowledge of the architectural data can help to understand the details of functionality during gestation and birth. The connective tissue architecture in the uterus of reproductive age is composed of three different layers. The first inner layer is a non-organized cluster-like interweaving of the fiber complex, secondly circular fibers in the middle layer and finally longitudinal fibers in the exterior layer[16]. In the postmenopausal uterus, the cervical region primarily includes well oriented longitudinal fibers[4].

Fiocchi *et al*[5], argued that two third of the caesarean scarred uteri had altered fiber structure in comparison to normal uteri in sutural zone. Numeric data of 13 volunteers (8 nulliparous- Ⅰ group, 5 with caesarean delivery- Ⅱ group) revealed lowest regional fiber number and density in the anterior isthmic portion (respectively 105, 77 and 9.3, 6.7), suture localization, especially in two patients with a big scar caused placental complication at subsequent delivery. The mean FA and ADC of the whole uterus were 0.4 ± 0.0 and 3.4 ± 0.4 × 10$^{-3}$ mm$^2$/s respectively. The ADC of group Ⅰ was higher than group Ⅱ, but not statistically significant. In this study they concluded that 3 T DTI may show *in-vivo* human uterine fiber structures and may detect significant caesarean scars which may lead to subsequent placental
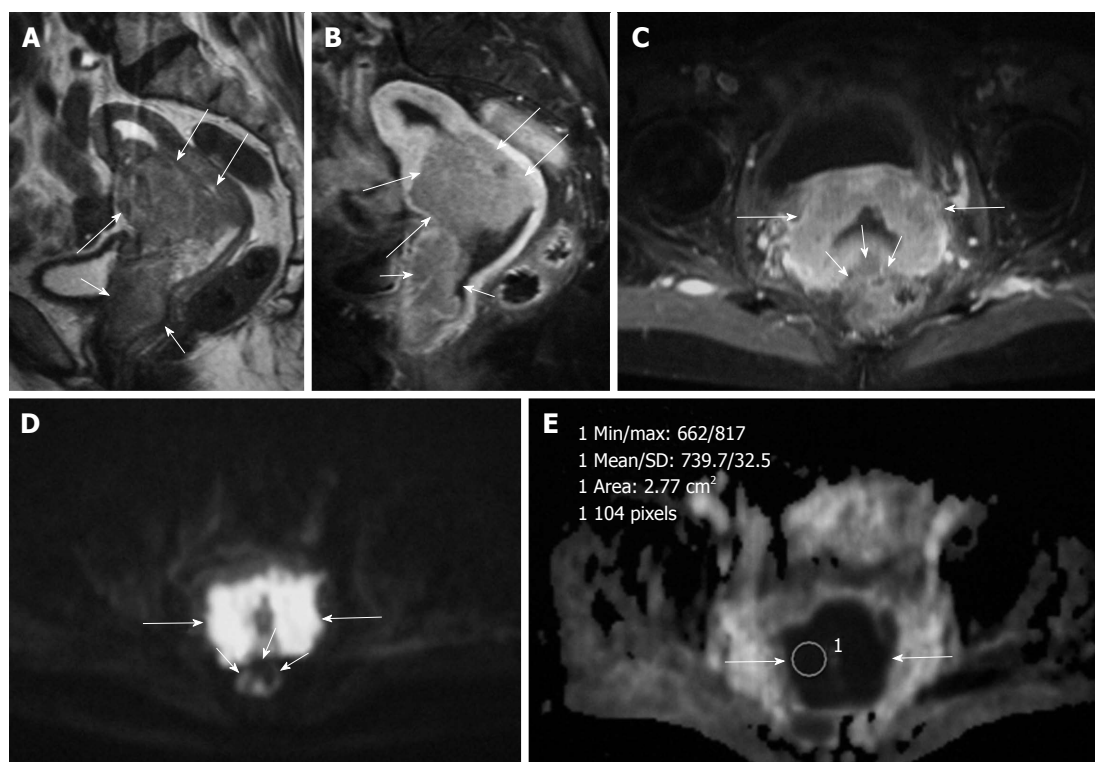
**Figure 1 Forty-three years old woman with stage III squamous cell carcinoma of the uterine cervix invading vagina.** A: Sagittal T2-weighted image of the uterus shows cervical cancer (long arrows) extending both to the corpus uteri and vagina (short arrows); B: Sagittal contrast-enhanced T1-weighted image with fat suppression shows enhancing cervical cancer (arrows). The tumor invades anterior vaginal wall (short arrows); C: Axial contrast-enhanced T1-weighted image with fat suppression shows enhancing cervical cancer (long arrows). There is suspicious invasion of the mass to the rectum (short arrows); D: Diffusion-weighted imaging with $b$ = 1000 s/mm$^2$ clearly shows a well-defined hyperintensity mass in the cervical area with no invasion to rectum (short arrows); E: On the apparent diffusion coefficient (ADC) map the tumor is hypointense (arrows). The ADC value within the mass is 0.73 × 10$^{-3}$ mm$^2$/s.

complications.

## DWI AND DTI OF DISEASED UTERUS

The addition of DWI, and DTI sequences which serve as functional imaging in the MRI protocol for the evaluation of uterine pathologies have been offered by several papers[2,3,7,8]. Besides quantitative evaluation with values has been found out to be effective in the discrimination of malignancy from benign lesions[17-20].

Owing to the amount of water and cellular density uterine zones exhibit different signal intensities on the DWI. The endometrial zone and cervix display high signal, however the myometrial zone reflects a lower signal and the junctional zone shows a very low signal. Kilickesmez *et al*[8] reported that the mean ADC values of the volunteers for myometrial zone 1.76 × 10$^{-3}$ mm$^2$/s, junctional zone 0.99 × 10$^{-3}$ mm$^2$/s, endometrial zone 1.65 × 10$^{-3}$ mm$^2$/s, and cervix as 1.71 × 10$^{-3}$ mm$^2$/s. Malignant lesions mostly display markedly high signal intensity on the DWI, due to water diffusion restriction in high cellular tissues of the malignant lesions[17,21].

Both DWI and DTI of the uterus is generally acquired in the axial slices, since the basic sequences of abdomen is in the axial plane, to decrease the acquisition time for covering whole pelvis along with the uterus.

DWI clearly detects the malignant tumors and metastic lymph nodes with high signal against suppressed background signal of normal tissues, and this sequence may be used like a positron emission tomography image for fast and accurate cancer detection[8] (Figure 1).

### Myometrial lesions
The most frequent lesions encountered in the myometrial zone are fibroids. These are benign overgrowths of uterine muscle, reported to be probably to be found in up to 70% of females of reproductive age[22].

Myometrial malignant lesions are leiomyosarcomas and stromal sarcomas[23]. Some of the benign fibroids, in association with different types of degeneration or cellular types may lead to high signal intensity on T2-weighted sequences. Thus, the discrimination of benign and malignant myometrial lesions are challenging on conventional MRI.

Tamai *et al*[24] reported that DWI may be an useful for discriminating uterine sarcomas from benign fibroids. The ADC values of normal myometrial zone and degenerated fibroids were higher than uterine sarcomas and there was no overlap; however, there was an overlap with non-degenerated and cellular fibroids[24]. Pathological examination of the large fibroids with central necrosis revealed fibrosis. This finding was consistent with isotropic diffusion in DTI of the associated lesion. Fibrotic leiomyomas include non-parallel collagen fibrils, whereas
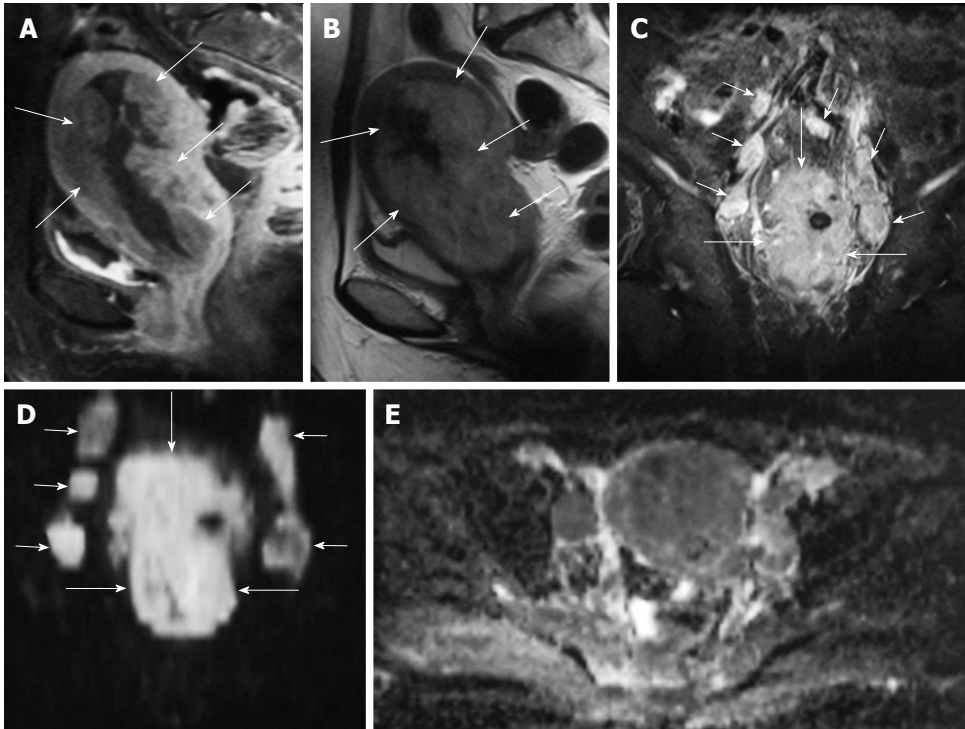
**Figure 2 A 57-year-old woman with endometrial carcinoma.** A: Sagittal contrast-enhanced T1-weighted image with fat suppression shows enhancing endometrial cancer with infiltration of myometrium (arrows); B: Sagittal T2-weighted image demonstrating hyperintense endometrial cancer with infiltration of myometrium (arrows); C: Coronal fat supressed T2-weighted image reveals a tumor in the corpus uteri (long arrows), and bilateral metastatic lymphadenopathies along the iliac chains (short arrows); D: Coronal DWI ($b$ = 1000 s/mm$^2$) shows a marked hyperintense tumor in the corpus uteri (long arrows), and bilateral metastatic lymphadenopathies along the iliac chains (short arrows); E: Axial apparent diffusion coefficient map reveals the right sided metastatic lymph node and endometrium with restricted diffusion.

there were well-structured collagen bundles neighbouring to smooth muscle cells in the normal myometrial zone[25,26]. Irregularity of these collagen bundles could be the reason for the lower degree of anisotropy in the fibroids when compared with the neighbouring myometrium.

The ADC values may also be beneficial for determining the therapeutic outcome after UAE, radiotherapy and/or chemotherapy[7]. The effect of UAE or focused ultrasound may be evaluated by the detection of ablated tissue with DWI. The ADC values of fibroids after treatment are lower when compared with initial ADC values[27,28].

### Endometrial lesions

The most frequent gynecologic malignancy is endometrial cancer. It should be discriminated from benign hyperplasia of the endometrium along with polyps.

The ADC value of polyps (1.27-1.58 × 10$^{-3}$ mm$^2$/s) and of normal endometrial zone (1.53 × 10$^{-3}$ mm$^2$/s) is significantly higher than endometrial cancer (0.88-0.98 × 10$^{-3}$ mm$^2$/s)[24,29] (Figures 2 and 3).

Histologic grade, stage, level of myometrium invasion, existence of nodal metastases, invasion of lymphoid and vascular structures all effect the prognosis of endometrial cancer. However the most important factor effecting prognosis is the depth of myometrium invasion[30]. The success of DWI has been improved in the assessment of accurate myometrium inavasion detection and in differentiating tumor recurrence from post-theraupetic findings[31]. The first surgical staging of endometrium cancer was proposed in 1988, and than the update of the International Federation of Gynecology and Obstetrics (FIGO) staging was done in 2009[32]. In this revised FIGO staging system, stage Ⅰ A tumors include the tumors invading solely the inner half of the myometrial zone and the tumors confined to endometrium[32,33]. Tumors infiltrating the exterior half of the myometrial zone are defined as stage Ⅰ B tumors. These revisions include simplification of stage Ⅰ disease and determination of cervical infiltration as a distinct stage to increase the diagnostic value of MRI[30].

According to Fujii *et al*[29], the ADC value was 84.6% successful in detecting endometrial cancer. Toba *et al*[2] investigated the feasibility of DTI for evaluating the myometrial invasion of endometrial cancer. The degree of myometrium invasion was subgrouped as stage E (confined to endometrial zone), more than 50%. The ADC values of the cancer, inner or exterior myometrial zones were not statistically different. Tumoral FA values (0.21 ± 0.05) were lower than the inner leyer of the myometrial zone (0.44 ± 0.01) and exterior myometrium (0.32 ± 0.08) ($P$ < 0.01). The inner or exterior myometrial FA values, (0.45 ± 0.05 *vs* 0.43 ± 0.04) were not statistically different in stage E cancers. However, in stage S and D tumors the FA values of the inner or exterior myometrial FA zones were significantly different (0.5 ± 0.05 *vs* 0.3 ± 0.04, $P$ < 0.01; 0.39 ± 0.03
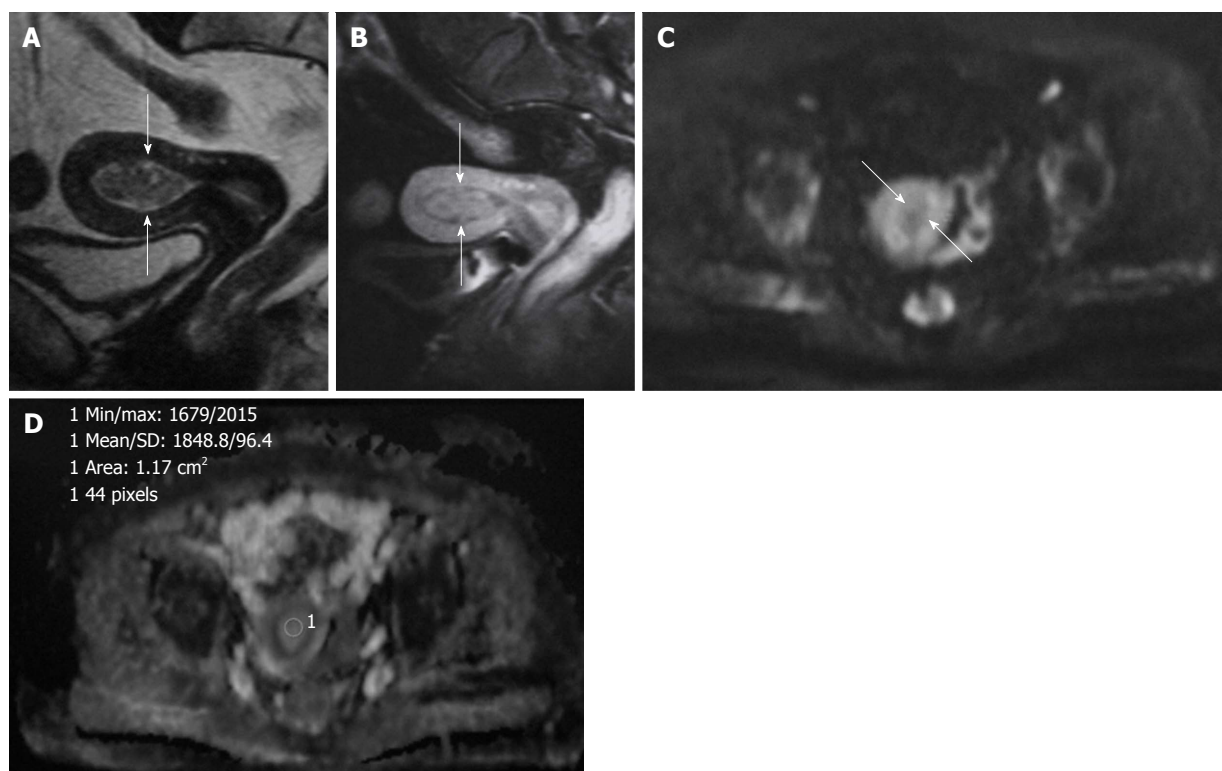
**Figure 3  A 42-year-old woman with endometrial polyp.** A: Hypointense polyp in the endometrial cavity on sagittal T2-weighted image mimicking low grade endometrial carcinoma (arrows); B: Sagittal contrast-enhanced T1-weighted image with fat suppression shows enhancing endometrial polyp (arrows); C: On the axial DWI ($b$ = 1000 s/mm$^2$) image, the mass is hypointense clearly excluding malignancy (arrows); D: Corresponding axial apparent diffusion coefficient (ADC) map. The ADC value within the mass is 1.85 × 10$^{-3}$ mm$^2$/s.
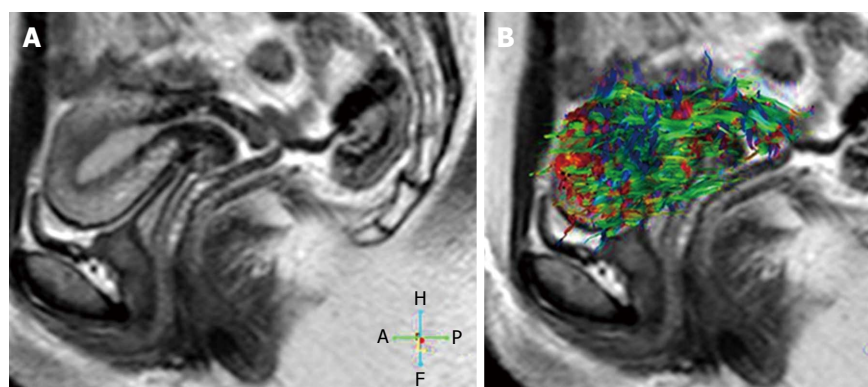


**Figure 4  Thirty two years old volunteer.** A: Sagittal T2-weighted image of a normal uterus; B: 3D whole tractography image of the normal uterus. Red colors represent a right-left orientation, blue represents a cranio-caudal orientation and green represents an antero-posterior orientation of diffusion. Changes in the intensity of the color represent different strengths of anisotropy.

*vs* 0.22 ± 0.01, *P* < 0.01; respectively). Myometrial infiltration of endometrial tumor may be detected with the disruption of the anisotropic layer.

DWI and DTI have a potential role for the discrimination of benign and malignant endometrial masses. It may also give additional information for preoperative assessment and should be performed as a part of routine MRI for endometrial tumors. Besides, DWI is a useful technique increasing the accuracy of staging[30].

### Cervical lesions
Cervical cancer is a common gynaecological tumor.

However, its incidence has decreased in developed countries as a result of screening with the Papanicolaou test (Pap smear), cervical cancer is still an important cause of tumor-related death in developing countries[34].

ADC measurements made significant supplement for the discrimination of normal cervical zone and cancers preoperatively. Besides there was correlation between tumor type, stage and ADC values[35].

According to McVeigh *et al*[36] the average median ADC of normal cervix was statistically higher than cervical cancers (2.09 × 10$^{-3}$ mm$^2$/s *vs* 1.09 × 10$^{-3}$ mm$^2$/s), and returned to the normal level following

chemotherapy and/or radiotherapy.

Kilickesmez *et al*[8] found out a statistically significant difference between the ADC values of malignant (0.88 ± 0.11) and benign (1.55 ± 0.33; *P* < 0.01) uterine lesions. In this study they reported a cut-off ADC level for malignant lesions at $1.05 \times 10^{-3}$ mm$^2$/s with a sensitivity, specificity, and accuracy of 95.83%, 94.55%, and 94.94%, respectively. This study demonstrated that quantitative DWI has the potential to discriminate normal and malignant lesions of the uterus.

However, correlation of DWI and DTI with reference sequences is essential for the reason that resolution is relatively low and normal structures such as lymph nodes, bowel loops, and hemorrhage, endometromas, may show high signal like cancers on DWI[8] (Figure 4). This phenomenon may lead to false-positive visual assessment. However, quantitative evaluation with ADC and FA values or correlation of DWI, DTI with reference sequences may overcome this[37].

Although not clearly proved like DWI (low ADC in malignant tumors), quantitative DTI also reveals difference in the FA value of benign *vs* malignant tissue, however statistical significance can be much more less detected. Besides there is confusion regarding FA value alterations which should be evaluated with further studies[2,38,39].

## CONCLUSION

According to this review, DWI and DTI emerge to be applicable and reliable sequences for the determination of physiological fluctuations of the uterus, detection of malignant lesions of the uterus and monitoring the therapeutic outcome. When combined with conventional MRI sequences, DWI and DTI provide further data about physiological and pathological conditions of the uterus. DWI and DTI are noninvasive, do not cause radiation exposure or need for contrast injection.

## REFERENCES

1    **Kido A**, Kataoka M, Koyama T, Yamamoto A, Saga T, Togashi K. Changes in apparent diffusion coefficients in the normal uterus during different phases of the menstrual cycle. *Br J Radiol* 2010; **83**: 524-528 [PMID: 20505034 DOI: 10.1259/bjr/11056533]
2    **Toba M**, Miyasaka N, Sakurai U, Yamada I, Eishi Y, Kubota T. Diagnostic possibility of diffusion tensor imaging for the evaluation of myometrial invasion in endometrial cancer: an ex vivo study. *J Magn Reson Imaging* 2011; **34**: 616-622 [PMID: 21751283 DOI: 10.1002/jmri.22693]
3    **Thrippleton MJ**, Bastin ME, Munro KI, Williams AR, Oniscu A, Jansen MA, Merrifield GD, McKillop G, Newby DE, Semple SI, Marshall I, Critchley HO. Ex vivo water diffusion tensor properties of the fibroid uterus at 7 T and their relation to tissue morphology. *J Magn Reson Imaging* 2011; **34**: 1445-1451 [PMID: 21953730 DOI: 10.1002/jmri.22793]
4    **Weiss S**, Jaermann T, Schmid P, Staempfli P, Boesiger P, Niederer P, Caduff R, Bajka M. Three-dimensional fiber architecture of the nonpregnant human uterus determined ex vivo using magnetic resonance diffusion tensor imaging. *Anat Rec A Discov Mol Cell Evol Biol* 2006; **288**: 84-90 [PMID: 16345078]
5    **Fiocchi F**, Nocetti L, Siopis E, Currà S, Costi T, Ligabue G, Torricelli

P. In vivo 3 T MR diffusion tensor imaging for detection of the fibre architecture of the human uterus: a feasibility and quantitative study. *Br J Radiol* 2012; **85**: e1009-e1017 [PMID: 22744322 DOI: 10.1259/bjr/76693739]
6    **Kuang F**, Ren J, Huan Y, Chen Z, Zhong Q. Apparent diffusion coefficients of normal uterus in premenopausal women with 3.0-T magnetic resonance imaging. *J Comput Assist Tomogr* 2012; **36**: 54-59 [PMID: 22261770 DOI: 10.1097/RCT.0b013e3182418885]
7    **Namimoto T**, Awai K, Nakaura T, Yanaga Y, Hirai T, Yamashita Y. Role of diffusion-weighted imaging in the diagnosis of gyneco-logical diseases. *Eur Radiol* 2009; **19**: 745-760 [PMID: 18839179 DOI: 10.1007/s00330-008-1185-5]
8    **Kilickesmez O**, Bayramoglu S, Inci E, Cimilli T, Kayhan A. Quantitative diffusion-weighted magnetic resonance imaging of normal and diseased uterine zones. *Acta Radiol* 2009; **50**: 340-347 [PMID: 19235579 DOI: 10.1080/02841850902735858]
9    **Wasnik AP**, Mazza MB, Liu PS. Normal and variant pelvic anatomy on MRI. *Magn Reson Imaging Clin N Am* 2011; **19**: 547-566; viii [PMID: 21816330]
10   **Brown HK**, Stoll BS, Nicosia SV, Fiorica JV, Hambley PS, Clarke LP, Silbiger ML. Uterine junctional zone: correlation between histologic findings and MR imaging. *Radiology* 1991; **179**: 409-413 [PMID: 1707545]
11   **Scoutt LM**, Flynn SD, Luthringer DJ, McCauley TR, McCarthy SM. Junctional zone of the uterus: correlation of MR imaging and histologic examination of hysterectomy specimens. *Radiology* 1991; **179**: 403-407 [PMID: 2014282]
12   **Brown MA**, Kubik-huch RA, Reinhold C. Uterus and cervix. In: Semelka RC, editor. 2nd edition, Abdominal pelvic MRI, vol. 1. New Jersey: John Wiley & Sons, Inc, 2006: 1251-1332
13   **Tsili AC**, Argyropoulou MI, Tzarouchi L, Dalkalitsis N, Koliopoulos G, Paraskevaidis E, Tsampoulas K. Apparent diffusion coefficient values of the normal uterus: Interindividual variations during menstrual cycle. *Eur J Radiol* 2012; **81**: 1951-1956 [PMID: 21621360 DOI: 10.1016/j.ejrad.2011.04.057]
14   **Longacre TA**, Bartow SA. A correlative morphologic study of human breast and endometrium in the menstrual cycle. *Am J Surg Pathol* 1986; **10**: 382-393 [PMID: 3717495]
15   **Fornasa F**, Montemezzi S. Diffusion-weighted magnetic resonance imaging of the normal endometrium: temporal and spatial variations of the apparent diffusion coefficient. *Acta Radiol* 2012; **53**: 586-590 [PMID: 22619357 DOI: 10.1258/ar.2012.110717]
16   **Dubrauszky V**, Schwalm H, Fleischer M. [The fibre system of connective tissue in the childbearing age, menopause, and pregnancy]. *Arch Gynakol* 1971; **210**: 276-292 [PMID: 5109671]
17   **Koyama T**, Togashi K. Functional MR imaging of the female pelvis. *J Magn Reson Imaging* 2007; **25**: 1101-1112 [PMID: 17520731]
18   **Ichikawa T**, Erturk SM, Motosugi U, Sou H, Iino H, Araki T, Fujii H. High-B-value diffusion-weighted MRI in colorectal cancer. *AJR Am J Roentgenol* 2006; **187**: 181-184 [PMID: 16794174]
19   **Nasu K**, Kuroki Y, Nawano S, Kuroki S, Tsukamoto T, Yamamoto S, Motoori K, Ueda T. Hepatic metastases: diffusion-weighted sensitivity-encoding versus SPIO-enhanced MR imaging. *Radiology* 2006; **239**: 122-130 [PMID: 16493012]
20   **Takahara T**, Imai Y, Yamashita T, Yasuda S, Nasu S, Van Cauteren M. Diffusion weighted whole body imaging with background body signal suppression (DWIBS): technical improvement using free breathing, STIR and high resolution 3D display. *Radiat Med* 2004; **22**: 275-282 [PMID: 15468951]
21   **Koh DM**, Collins DJ. Diffusion-weighted MRI in the body: applications and challenges in oncology. *AJR Am J Roentgenol* 2007; **188**: 1622-1635 [PMID: 17515386]
22   **Tropeano G**, Amoroso S, Scambia G. Non-surgical management of uterine fibroids. *Hum Reprod Update* 2008; **14**: 259-274 [PMID: 18344356 DOI: 10.1093/humupd/dmn006]
23   **Goto A**, Takeuchi S, Sugimura K, Maruo T. Usefulness of Gd-DTPA contrast-enhanced dynamic MRI and serum determination of LDH and its isozymes in the differential diagnosis of leiomyosarcoma from degenerated leiomyoma of the uterus. *Int J*

*Gynecol Cancer* 2002; **12**: 354-361 [PMID: 12144683]

24  **Tamai K**, Koyama T, Saga T, Morisawa N, Fujimoto K, Mikami Y, Togashi K. The utility of diffusion-weighted MR imaging for differentiating uterine sarcomas from benign leiomyomas. *Eur Radiol* 2008; **18**: 723-730 [PMID: 17929022]

25  **Catherino WH**, Leppert PC, Stenmark MH, Payson M, Potlog-Nahari C, Nieman LK, Segars JH. Reduced dermatopontin expression is a molecular link between uterine leiomyomas and keloids. *Genes Chromosomes Cancer* 2004; **40**: 204-217 [PMID: 15139000]

26  **Leppert PC**, Baginski T, Prupas C, Catherino WH, Pletcher S, Segars JH. Comparative ultrastructure of collagen fibrils in uterine leiomyomas and normal myometrium. *Fertil Steril* 2004; **82** Suppl 3: 1182-1187 [PMID: 15474093]

27  **Jacobs MA**, Herskovits EH, Kim HS. Uterine fibroids: diffusion-weighted MR imaging for monitoring therapy with focused ultrasound surgery--preliminary study. *Radiology* 2005; **236**: 196-203 [PMID: 15987974]

28  **Liapi E**, Kamel IR, Bluemke DA, Jacobs MA, Kim HS. Assessment of response of uterine fibroids and myometrium to embolization using diffusion-weighted echoplanar MR imaging. *J Comput Assist Tomogr* 2005; **29**: 83-86 [PMID: 15665689]

29  **Fujii S**, Matsusue E, Kigawa J, Sato S, Kanasaki Y, Nakanishi J, Sugihara S, Kaminou T, Terakawa N, Ogawa T. Diagnostic accuracy of the apparent diffusion coefficient in differentiating benign from malignant uterine endometrial cavity lesions: initial results. *Eur Radiol* 2008; **18**: 384-389 [PMID: 17917730]

30  **Beddy P**, O'Neill AC, Yamamoto AK, Addley HC, Reinhold C, Sala E. FIGO staging system for endometrial cancer: added benefits of MR imaging. *Radiographics* 2012; **32**: 241-254 [PMID: 22236905]

31  **Sala E**, Rockall A, Rangarajan D, Kubik-Huch RA. The role of dynamic contrast-enhanced and diffusion weighted magnetic resonance imaging in the female pelvis. *Eur J Radiol* 2010; **76**: 367-385 [PMID: 20810230]

32  **Creasman W**. Revised FIGO staging for carcinoma of the endometrium. *Int J Gynaecol Obstet* 2009; **105**: 109 [PMID: 19345353]

33  **Odicino F**, Pecorelli S, Zigliani L, Creasman WT. History of the FIGO cancer staging system. *Int J Gynaecol Obstet* 2008; **101**: 205-210 [PMID: 18199437]

34  **Solomon D**, Breen N, McNeel T. Cervical cancer screening rates in the United States and the potential impact of implementation of screening guidelines. *CA Cancer J Clin* 2007; **57**: 105-111 [PMID: 17392387]

35  **Demirbaş T**, Cimilli T, Bayramoğlu S, Güner NT, Hocaoğlu E, Inci E. Contribution of diffusion-weighted imaging to diagnosis and staging of cervical cancer. *Balkan Med J* 2014; **31**: 154-157 [PMID: 25207188]

36  **McVeigh PZ**, Syed AM, Milosevic M, Fyles A, Haider MA. Diffusion-weighted MRI in cervical cancer. *Eur Radiol* 2008; **18**: 1058-1064 [PMID: 18193428 DOI: 10.1007/s00330-007-0843-3]

37  **Shen SH**, Chiou YY, Wang JH, Yen MS, Lee RC, Lai CR, Chang CY. Diffusion-weighted single-shot echo-planar imaging with parallel technique in assessment of endometrial cancer. *AJR Am J Roentgenol* 2008; **190**: 481-488 [PMID: 18212236 DOI: 10.2214/AJR.07.2155]

38  **Li C**, Chen M, Li S, Zhao X, Zhang C, Liu M, Zhou C. Diffusion tensor imaging of prostate at 3.0 Tesla. *Acta Radiol* 2011; **52**: 813-817 [PMID: 21586608 DOI: 10.1258/ar.2011.100487]

39  **Kinoshita M**, Hashimoto N, Goto T, Kagawa N, Kishima H, Izumoto S, Tanaka H, Fujita N, Yoshimine T. Fractional anisotropy and tumor cell density of the tumor core show positive correlation in diffusion tensor magnetic resonance imaging of malignant brain tumors. *Neuroimage* 2008; **43**: 29-35 [PMID: 18672074 DOI: 10.1016/j.neuroimage.2008.06.041]